Giulia Di Rocco, Fabrizio Bernini, Marco Borsari, Ilaria Martinelli, Carlo Augusto Bortolotti, Gianantonio Battistuzzi, Antonio Ranieri, Monica Caselli, Marco Sola, and Glauco Ponterini*

Excitation-Energy Transfer Paths from Tryptophans to Coordinated Copper Ions in Engineered Azurins: a Source of Observables for Monitoring Protein Structural Changes

DOI 10.1515/zpch-2015-0749
Received December 14, 2015; accepted March 30, 2016

Abstract: The intrinsic fluorescence of recombinant proteins offers a powerful tool to detect and characterize structural changes induced by chemical or biological stimuli. We show that metal-ion binding to a hexahistidine tail can significantly broaden the range of such structurally sensitive fluorescence observables. Bipositive metal-ions as Cu^{2+}, Ni^{2+} and Zn^{2+} bind 6xHis-tag azurin and its 6xHis-tagged R129W and W48A-R129W mutants with good efficiency and, thereby, quench their intrinsic fluorescence. Due to a much more favourable spectral overlap, the 6xHis-tag/Cu^{2+} complex(es) are the most efficient quenchers of both W48 and W129 emissions. Based on simple Förster-type dependence of energy-transfer efficiency on donor/acceptor distance, we can trace several excitation-energy transfer paths across the protein structure. Unexpected lifetime components in the azurin 6xHis-tag/Cu^{2+} complex emission decays reveal underneath complexity in the conformational landscape of these systems. The new tryptophan emission quenching

***Corresponding author: Glauco Ponterini,** Department of Life Sciences, University of Modena and Reggio Emilia, Via Campi 103, I-41125 Modena, Italy, e-mail: glauco.ponterini@unimore.it
Fabrizio Bernini, Marco Borsari, Gianantonio Battistuzzi, Monica Caselli: Department of Chemical and Geological Sciences, University of Modena and Reggio Emilia, via Campi 103, I-41125 Modena, Italy
Giulia Di Rocco, Ilaria Martinelli, Antonio Ranieri: Department of Life Sciences, University of Modena and Reggio Emilia, Via Campi 103, I-41125 Modena, Italy
Carlo Augusto Bortolotti, Marco Sola: Department of Life Sciences, University of Modena and Reggio Emilia, Via Campi 103, I-41125 Modena, Italy; and CNR-NANO Institute of Nanoscience, Via Campi 213/A, I-41125 Modena, Italy

paths provide additional signals for detecting and identifying protein structural changes.

Keywords: Excitation-Energy Transfer, Tryptophan Fluorescence, Protein Intrinsic Fluorescence, Azurin, Coordinated Copper Ion.

1 Introduction

Intrinsic protein fluorescence represents a rich source of structural information [1–3]. It can provide a number of structure-related observables to be exploited in label-free fluorescence experiments on recombinant proteins, thus avoiding the problems associated with extrinsic fluorescent probes [1, 4]. Changes in the structural determinants of the tryptophan (more rarely tyrosine) fluorescence properties, i. e., spectra, intensities, lifetimes and anisotropies, can result from binding of a protein to small ligands or to biological macromolecules, proteins or nucleic acids in, e. g., drug/target interaction studies or model experiments aimed at unraveling the biological interactors of a key protein. Such structural changes can be monitored in *in-vitro* experiments and can be identified if the observed changes in the overall fluorescence response of the recombinant protein can be assigned to specific tryptophan residues [2, 3]. Among the processes modulated by the protein structural changes, electron and energy transfers, with their high sensitivity to the distance between the partners, are often involved. However, while electron transfer is a short-distance, few Angström phenomenon, Förster-type energy transfer can occur over few nanometers. Thus, it offers a larger spectrum of structure-related energy-transfer efficiencies that can be exploited to deduce structural information [1]. On the other hand, because tryptophan is the lowest excitation-energy chromophore in proteins, energy transfer from tryptophan residues requires introduction of external quenchers. In this contribution, we propose to take advantage of the widespread attachment of polyhistidine tags to recombinant proteins for purification purposes to easily increase the number of tryptophan quenching paths in a protein of interest. We show that this is readily achieved in three engineered his-tagged azurins by complexation of several bipositive metal ions at a 6xHis-tag.

Azurin is a small blue copper protein that acts as an electron carrier in a variety of denitrifying bacteria [5]. Recombinant wild type azurin consists of 148 aminoacids, 20 of which forming the signal peptide sequence, with a single tryptophan residue (Trp48), whose indole sidechain lies buried inside the protein hydrophobic core (Figure 1). Hence, upon excitation at 280–300 nm, the protein features a structured ^1L_b fluorescence emission spectrum with a maximum

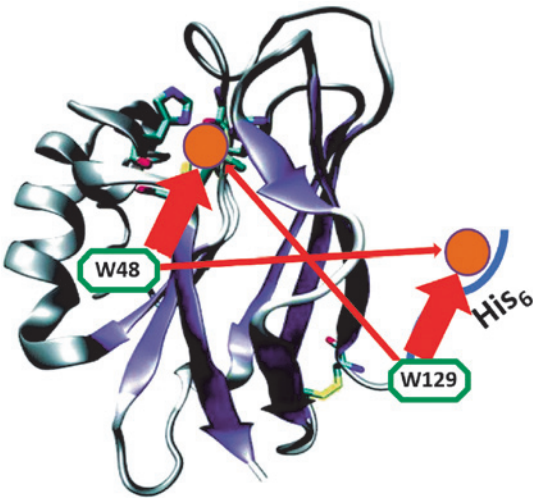

Figure 1: Schematic representation of the investigated azurins. Cu^{2+} ions bound to the 6xHis-tag and at the T1-site are represented by orange balls. The main energy-transfer paths recognized are shown by straight arrows. Thicker arrows indicate faster energy transfers.

at 306–308 nm, which is typical of the emission of an indole ring surrounded by a non-polar environment ([1] and references therein). The type-1 (T1) copper ion of the holoprotein has a marked quenching effect on the emission of the buried tryptophan residue, since the emission quantum yield of the apoprotein is more than five times larger than that of the WT protein [6–8]). Time-resolved emission decay analyses of azurin have found one [7, 9, 10] or two [11–13] short lived decay components, with lifetimes usually around 0.1–0.2 ns, though a 0.5–0.6 ns component has been reported [11, 13]. Additionally, a 4.5–4.9 ns component is usually found with fractional contribution changing from work to work. The origin of the short-lived component(s), and the related observation of a surviving longer-lived one, have been the subject of a still unsettled debate. The short-lived component has been connected with the existence of a conformation of the enzyme in which Trp48 is quenched by the T1-site copper ion. Based on spectroscopic and XRD structural data, this quenching has been attributed either to energy transfer mediated by copper-histidine charge-transfer states responsible for transitions with significant oscillator strength and spectral overlap with the Trp48 emission band, or to electron transfer [9]. From the decay analysis of apoazurin, a single component with a 4.7–5.1 ns lifetime [13], the efficiency of the quenching process yielding this short-lived component is about 0.96. A first hint at the complexity of the problem is provided by the observation that the ratio of the long-to-short lifetimes, about 20–30, is much larger than the above given ratio of the emission quantum yields of the apo- and holoazurins, i. e., 5–6. The surviving ~ 4.7 ns component has been attributed to a fraction of apoprotein [9]. However, an azurin featuring a 4.5 ns lifetime has

been later shown to differ from the apoprotein in terms of structural resistance to a chaotropic agent [10], thus indicating the existence of a conformation of holoazurin in which the Trp48 emission is not strongly quenched by the T1-copper ion complex. These studies highlight the conformational heterogeneity of this protein.

Histidine and proteins containing histidine-rich domains play a critical role in many life functions such as copper transportation in both prokaryote and eukaryote organisms. Hence, the increased interest in the understanding of the binding mode(s) and of the thermodynamic properties of physiological metal(II)-histidine species [14, 15]. A useful tool for mimicking these histidine- and polyhistidine-metal complexes *in vitro* are N- or C-terminal hexa-histidine tags (6xHis-tags) fused to recombinant proteins [16, 17]. These systems owe their popularity to their special metal-ion binding properties and their ability to avoid interference with protein folding and biological functionality of the proteins [16, 17]. Because of the widespread use of His-tags for protein purification, extensive studies have been performed on copper, zinc, and nickel ion binding to His-containing model peptides. These revealed that bipositive metal ions most likely bind two non-consecutive imidazoles and a pH-dependent number of amide nitrogens [15, 18]. Moreover, experimental and computational studies suggest the existence of polymorphic binding states for the complexes formed by Cu^{2+} with the Ac-$(His)_6$-NH_2 peptide, as the metal ion can bind the imidazole sidechains of various pairs of histidines with different efficiencies [15]. However, little is known about the metal-ion binding properties of protein-bound His-tag domains.

This work aims at showing that modulation of intrinsic tryptophan fluorescence properties of His-tagged azurins can be achieved by transition metal-ion, especially Cu^{2+}, binding at fused polyhistidine tags, thus broadening the range of fluorometric observables from which structurally relevant information can be deduced. We have characterized the efficiency of the 6xHis-tag fused to the C-terminal of the three azurins to chelate copper and other transition metal ions, an essential property for a model of physiological histidine-transition metal complexes. Additionally, because of the known ability of azurin to cross the cellular membrane [19], these azurin 6xHis-tag systems might be adapted to become efficient and versatile physiological metal-ion carriers.

2 Experimental

2.1 Protein production and isolation

Pseudomonas aeruginosa WT azurin containing a C-terminal six-residue-long polyhistidine-tag (6xHis-tag) was produced and purified following the procedure described elsewhere [20]. The QuikChange XL site-directed mutagenesis kit (Agilent Technologies) was used for the Arg to Trp substitution in position 129 and for the further Trp to Ala mutation of residue 48, starting from the synthetic oligonucleotide primers carrying the desired mutations, namely: R129WF: 5'-accctgaccctgaagtggatccatcaccatcac-3' R129WR: 5'-tgatggtgatggatccacttcagggtcagggt-3'; W48AF: 5'-gtcatgggccacaacgcggtactgagcaccgcc-'3 and W48AR: 5'-ggcggtgctcagtaccgcgttgtggcccatgac-'3. The p3AZU-PAOH plasmid that expresses the wt *azurin* fused to a C-terminal six-residues- polyhistidine-tag (6xHis-tag) [20] was used as a template in the production of the W48A/R129W mutant as reported above.

The WTAzu, R129WAzu and W48A/R129WAzu variants were expressed in *E. coli* DH5α cells using LB medium containing 1 mM $CuCl_2$. The expression was induced by addition of 0.5 mM IPTG. The periplasmic fraction containing azurin was prepared following published procedures [21]. The proteins were purified using metal affinity chromatography (HisTrap, Amersham Biosciences), concentrated up to 10^{-4} M and stored in 50 mM sodium acetate, pH 5.

2.2 UV-vis and fluorometric experiments

Absorption spectra were recorded with a JASCO UV-Vis spectrophotometer equipped with a 1 cm quartz cell. Steady-state fluorescence measurements were carried out with a JASCO FP 6200 or a Horiba Jobin-Yvon FluoroMax3 spectrofluorometers. The excitation and emission spectra were corrected for the lamp emission spectrum and the detector response spectral sensitivities. In order to minimize protein aggregation and inner-filter effects, protein concentrations were kept lower than 3 μM (absorbances at 280 nm were lower than 0.1). Measurements were performed in 10 mM HEPES buffer and 50 mM NaCl at pH 6.8. For the determination of the emission quantum yields, the WT protein, (Φ_f = 0.054, the mean of the two reported quantum yield values, 0.052 [7] and 0.056 [11]) was used as the reference for the buried tryptophan emission, while d-tryptophan in water (Φ_f = 0.13 [1]) was the standard for the exposed tryptophan emission. The latter

also served for the determination of the W48A/R129W protein emission quantum yield.

2.3 Fluorescence time-resolved measurements

Fluorescence decays were measured with a Horiba FluoroMax4 equipment, employing a 295 nm LED excitation source. The instrument response function was approximately 1 ns and was reduced to about 0.1 ns after deconvolution. The peak channel in the decays contained 10^4 counts and at least two decays were measured at each emission wavelength. Fluorescence decays were fit to a sum of exponentials, and an adequate fit had a x^2 between 1.00 and 1.20. The smallest number of components that provided an acceptable fit was used. The complex emission decay profiles of the two-tryptophan R129W azurin were analyzed with guidance from the single-tryptophan protein results, using some of their characteristic lifetimes as fixed parameters in 4 or 5 exponential fittings. Measurements were carried out at 22 ± 2 °C on protein samples all characterized by an absorbance of 0.1 over a 1 cm pathlength at 280 nm. For a given component, under the assumption that its fractional contribution, f, was wavelength independent across the emission spectrum, we estimated the radiative and the radiationless decay rate constants, k_r and k_{nr}, as $k_r = f\Phi_f/\tau$ and $k_{nr} = (1 - f\Phi_f)/\tau$, where Φ_f is the overall emission quantum yield and τ the specific lifetime.

2.4 Fluorometric analysis of metal ion/azurin his-tag binding equilibrium

The affinity constants of WT, R129W and W48A/R129W His-tagged azurins for transition metal ions (Cu^{2+}, Ni^{2+}, Zn^{2+}, and Cr^{3+}) were determined by titrating known amounts of the oxidized proteins (sample volume: 2.0 mL, protein concentration: 3.0×10^{-6} M) in 10 mM Hepes buffer containing 50 mM NaCl, at pH = 6.8, with metal ion solutions of known concentrations prepared in the same buffer. We followed the changes induced in the emission spectra of the protein tryptophans upon 290 nm excitation. To make sure we were measuring equilibrium intensity values, we either repeated each measurement more times until a stable value was obtained, or interrupted the titration and checked that the last value was re-obtained one or two hours later or, finally, checked that the results of the titration did not significantly change if consecutive metal-ion additions were separated by different time intervals.

The measured fluorescence intensities at 310 and 350 nm were corrected for the increase in absorbance at these wavelengths due to the added metal ion, as $I = I_{meas} \times 10^{(A_{290}+A_{em})/2}$. Here, I_{meas} is the measured intensity, A_{290} the increase in absorbance at the excitation wavelength, 290 nm, due to the metal ion added, and A_{em} the corresponding increase in absorbance at the emission wavelength, 310 or 350 nm. These corrections account for the decrease in intensity of the exciting beam and the reabsorption of the emitted light due to the added metal ions, both approximately described in terms of a 0.5 cm path.

Under the assumption of a 1 : 1 metal/6xHis-tag binding stoichiometry, the dissociation constant of the metal-protein adducts, K_d, were determined by fitting the observed changes in protein emission intensity, I, as a function of metal-ion concentration, $[M]$, with Equation (1)

$$I = \frac{K_d I_0 + [M] I_\infty}{(K_d + [M])} \quad (1)$$

where I_0 and I_∞ are the protein emission intensities in the absence of metal ion and at saturation of the 6xHis-tag (see the supplementary material for a derivation of Equation (1)).

3 Results and discussion

3.1 Steady-state fluorescence properties of Trp48 and Trp129

We have studied the influence that binding of Cu^{2+}, Ni^{2+}, Zn^{2+} and Cr^{3+} ions to a C-terminal 6xHis-tag exerts on steady-state and time-resolved intrinsic fluorescence of wild type *Pseudomonas aeruginosa* azurin, as well as that of its R129W and W48A/R129W variants. In the former mutant, a second tryptophan (Trp129), introduced just before the beginning of the 6xHis-tag, increases the variety of the fluorescence observables and the sensitivity of the fluorometric detection of metal-ion binding by providing an additional energy-transfer donor for the His-tag/metal ion complexes (Figure 1). The double mutant W48A/R129W allows the individual fluorescence properties of Trp129 to be investigated and characterized without interference from Trp48, and offers an additional model putatively characterized by high fluorescence sensitivity to metal-ion binding to the nearby 6xHis-tag.

The fluorescence excitation and emission spectra of the single-tryptophan azurins, WT and the W48A/R129W mutant, and of the two-tryptophan R129W variant, are collected in Figure 2. The emission and excitation spectra of the R129W protein depend on the excitation and emission wavelengths, respectively,

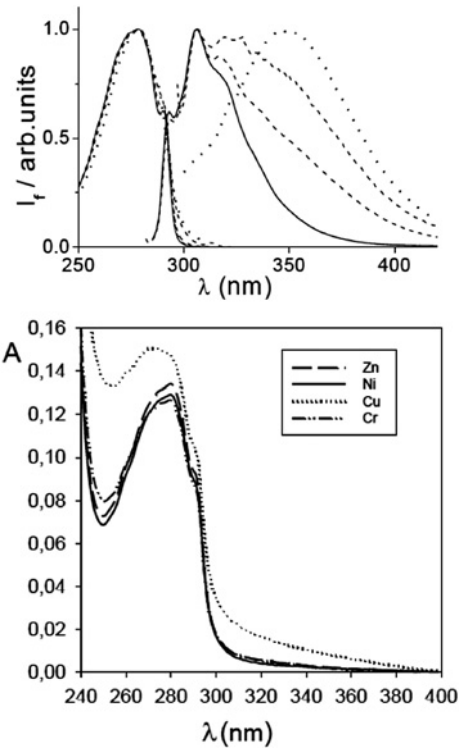

Figure 2: Top: excitation and emission fluorescence spectra of the three azurins. WT: solid lines, λ_{exc} = 270 nm, λ_{em} = 320 nm. W48A/R129W: dotted lines, λ_{exc} = 290 nm, λ_{em} = 340 nm. R129W: dashed lines, λ_{exc} = 280 and 295 nm, in order of increasing emission intensity at 350 nm; λ_{em} = 305, 320, 350 nm, in order of increasing intensity of the excitation spectra at 300 nm. pH 6.8. Bottom: UV-Vis absorption spectra of R129W azurin in the presence of 10 μM of the reported metal ions. The spectra were recorded at 20 °C using 3.0 μM protein samples in 10 mM HEPES buffer and 50 mM NaCl at pH 6.8. Abs = absorbance. The optical path was 1 cm.

as expected because of the two tryptophan fluorophores having different absorption and emission spectra. The buried tryptophan, Trp48, features a structured ^1L_b emission spectrum with maximum at 306 nm, very similar to those exhibited by the Trp48 of the WT protein [1]. Conversely, Trp129 features a broad ^1L_a emission spectrum with maximum at 350 nm, typical of an exposed tryptophan [1], both in the R129W single mutant and in the W48A/R129W double mutant, an exposure consistent with the peripheral position of the 129 residue.

In order to evaluate the quantum yields of the two tryptophans in the R129W variant, we determined their individual absorption and emission spectra. The emission spectrum of the exposed tryptophan was obtained from the total emission spectrum of the R129W protein after subtraction of the WT azurin emission spectrum, multiplied by a numerical factor, determined by trial and error, such that the resulting difference would show no recollection of the vibronic structure of the WT spectrum. An example of this procedure is shown in Figure S1, in the supplementary material. The Trp129 spectrum of the two-tryptophan protein thus obtained is very similar to the emission spectrum of the Trp129 in the single-tryptophan W48A/R129W variant, shown as a dotted line in Figure 2. The

Table 1: Fluorescence emission quantum yields of individual tryptophan residues in R129W and W48A/R129W azurins at 22 °C.

R129W buried	0.062 ± 0.015
R129W exposed	0.10 ± 0.03
W48A/R129W	0.095 ± 0.010

latter includes an unstructured, broad emission with maximum around 300 nm, likely due to tyrosine emission unquenched by the peripheral Trp129. The relative absorptions of the two tryptophan residues were obtained by fitting the higher-wavelength portion of the absorption band of the R129W mutant as the sum of properly scaled excitation spectra of the single-tryptophan WT protein and of the two-tryptophan R129W protein measured at $\lambda_{em} = 350$ nm, a wavelength at which emission is almost completely due to the exposed tryptophan.

The individual spectra thus obtained were employed to determine the emission quantum yields of the two tryptophans of R129W. The absorption spectra provided the fractions of incident photons absorbed by each residue at the wavelength of the experiment. The results (Table 1) indicate that the emission quantum yield of the buried tryptophan residue of R129W coincides with that of the WT azurin tryptophan (0.052 [7], 0.056 [11]) within our experimental error. As for the exposed Trp129, its quantum yields in R129W and W48A/R129W are very similar to each other and about 1.5 times larger than that of the buried, Trp48 residue. The latter finding represents a starting advantage in view of obtaining well measurable fluorescence quenching following metal-ion binding. Overall, these results imply a negligible quenching of the buried Trp48 emission by the exposed Trp129.

3.2 Time-resolved intrinsic fluorescence properties

Time-resolved experiments yielded a two-component emission decay from the buried Trp48 of the WT protein, with lifetimes around 0.2 and 4.6 ns (Figure 3 and Table S1 in the supplementary material), consistent with published data for the same protein ([10, 13] and references therein). From the fractional contributions of the two components, $f_{1,2}$, and the quantum yields, Φ_f, and lifetimes, τ_1, reported in Tables 1 and S1 and in Figure 3, we obtain $k_{r1} = 1.0(\pm 0.5) \times 10^7\ s^{-1}$ and $k_{nr1} = 5(\pm 1) \times 10^9\ s^{-1}$ (details are in the experimental section). The longer-lived component is characterized by a $k_{r2} = k_{r1} = 1.0(\pm 0.1) \times 10^7\ s^{-1}$ and $k_{nr2} = 2.0(\pm 0.2) \times 10^8\ s^{-1}$. Whether we assume the unquenched Trp48 lifetime to correspond to our longer-lived component [9], or we take it equal to the average of the

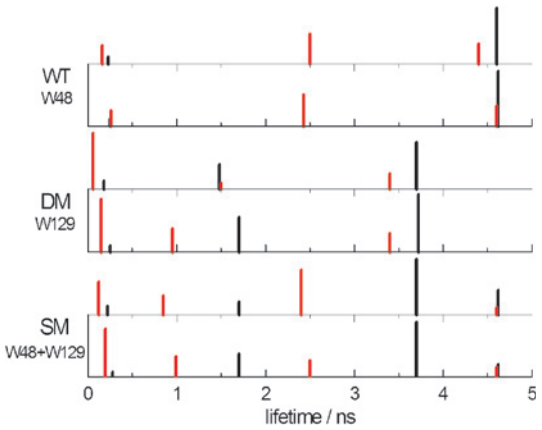

Figure 3: Lifetimes obtained from emission decay multiexponential fitting of the WT and the W48A/R129W (DM) and R129W (SM) azurins in the absence (black) and presence (red, 100 μM) of exogenous Cu^{2+} ions. Each bar height is proportional to the fractional contribution of the lifetime component. For each protein, the upper set (lighter axis) represents results obtained at shorter wavelengths (320 or 330 nm), the lower one at longer wavelengths (350 or 370 nm).

Table 2: Quenching rate constants (k_q) deduced from time-dependent measurements without and with (*) 50 μM copper ion, suggested donors and acceptors and relative distances (r_{DA}) determined or estimated (#) from XRD structures of WT azurin (PDB entry 1AZU; [22]) and a histidine triad/Zn complex [23]. T1-Cu = T1-site/Cu complex; HT-Cu = 6xHis-tag/Cu complex. r^o_{DA} is an estimated Förster critical distance. Confidence intervals, estimated from the uncertainties on the source data (see text), are given within parentheses.

$k_q/10^8\ s^{-1}$	donor	acceptor	r_{DA} , r^o_{DA}/Å
50(±10)	$W48^{WT}$	T1-Cu	8.1
27(±6)	$W129^{W48A/R129W}$		
3.3(±0.6)	$W129^{W48A/R129W}$	T1-Cu	27.6, 30
2(±0.4)	$W48^{WT}$ *	HT-Cu	> 21 #
50(±20)	$W48^{WT}$ *		
60(±10)	$W129^{W48A/R129W}$ *	HT-Cu	< 8 #
4–7	$W129^{W48A/R129W}$ *		

lifetimes reported for the apoprotein, 4.9 ns [10, 11], we estimate the quenching rate constant in this protein to hold $k_q^{WT} = k_{nr1} - k_{nr2} = 5(\pm1) \times 10^9\ s^{-1}$ (Table 2).

The emission decay of the W48A/R129W double mutant, that only contains the exposed Trp129, was well fit using three components, 0.3, 1.7 and 3.7 ns. The longest lifetime is quite typical of a highly exposed, unquenched tryptophan [1]. The shorter components likely result from energy transfer from the engineered Trp129 to the T1-site copper ion and suggest the existence of two conformations of the mutated protein characterized by different quenching constants. The corresponding radiative and radiationless decay rate constants, calculated as for the components of the WT protein decay, hold $k_{r1} = 2(\pm1) \times 10^7\ s^{-1}$, $k_{r2} = 1.7(\pm0.5) \times 10^7\ s^{-1}$, $k_{r3} = 1.5(\pm0.3) \times 10^7\ s^{-1}$, $k_{nr1} = 3.3(\pm0.6) \times 10^9\ s^{-1}$,

$k_{nr2} = 5.7(\pm0.5) \times 10^8\ s^{-1}$ and $k_{nr3} = 2.5(\pm0.2) \times 10^8\ s^{-1}$. The mean radiative rate constant is thus about twice that of the Trp48 decay, in keeping with the higher oscillator strength of the S_0-^1L_a relative to the S_0-^1L_b transitions [1]. From the non-radiative rate constant values, we estimate the two quenching rate constants to hold $k_{q1}^{W48A/R129W} = k_{nr1} - k_{nr3} = 2.7(\pm0.6) \times 10^9\ s^{-1}$ and $k_{q2}^{W48A/R129W} = k_{nr2} - k_{nr3} = 3.3(\pm0.6) \times 10^8\ s^{-1}$, i. e., respectively, about 2 and 15 times smaller than the corresponding quenching rate constant of Trp48 (Table 2). The 1.7 ns component, resulting from the k_{q2} rate constant, corresponds to a quenching efficiency of 0.54, much smaller than for the short-lived component of the WT protein decay. This is consistent with the increased distance between Trp129 and the T1-copper complex relative to the Trp48/T1-copper complex of WT azurin, 27.6 vs 8.1 Å in the XRD structure of WT azurin [22]. 30 Å thus represents a reasonable estimate of the Förster critical distance for the tryptophan/T1-Cu^{2+} donor/acceptor pair. The shortest-lived component is responsible for the marked decrease in the amplitude-weighted lifetime of the double mutant relative to the WT protein, 1.6(±0.4) vs 2.5(±0.4) ns (Table S1), and must result from a yet unidentified high-efficiency (0.92) quenching of Trp129.

The emission decay of the two-tryptophan mutant, R129W, is an emission-wavelength-dependent superposition of the decays of the two single-tryptophan protein emission decays. Consistently with residue exposition and the steady-state emission spectra in Figure 2, the Trp48, 4.7 ns component features higher fractional contributions at 320 and 330 nm, while the Trp129, 1.7 ns component of the decay shows higher contributions at longer emission wavelengths. The excellent fits of the complex decays of this protein obtained by employing some of the lifetimes of the single-tryptophan proteins as fixed parameters confirms the lack of interaction between the two tryptophans already suggested by the close similarity of the Trp48 emission quantum yields in WT and R129W azurins.

3.3 Metal-ion binding to the 6xHis-tagged azurins

3.3.1 UV-visible spectra

The UV-visible absorption spectra of WT, R129W and W48A/R129W His-tagged azurins feature two main peaks located at 280 and 628 nm, typical of azurin [5]. The former is the classical aromatic band of proteins, while the latter is typical of a type-1 blue copper protein and is assigned to the LMCT transition $(S(Cys - \pi) \rightarrow Cu(II)_{dx2-y2})$, involving the copper atom of the active site and Cys112 [24, 25]. The effect of Cu^{2+}, Ni^{2+}, Zn^{2+} and Cr^{3+} binding to the C-terminal 6xHis-tag on the UV-vis absorption spectra of WT, R129W and W48A/R129W

azurins was analyzed by recording the UV-vis spectra of the two proteins in the presence of increasing concentrations of the metal ions, up to a 15 : 1 metal ion/protein concentration ratio. The spectra between 240 and 420 nm of R129W azurin in the presence of some of the metal ions are reported in Figure 2. The band at 628 nm, due to the copper ion of the protein active site, did not change, demonstrating that the T1 copper site was unaffected by metal binding to the C-terminal 6xHis-tag (data not shown). Notably, following addition of Cu^{2+} ions, the spectrum showed an absorption increase in the 300–350 nm region, which has been previously observed for hexapeptide/Cu^{2+} complexes [15, 26] and for various blue oxidases containing a type 3 copper center [27–29]. In all cases, the copper ion was coordinated by the imidazole rings of two or three histidines while the remaining coordinating positions were free or occupied by solvent molecules. $N_{im} \rightarrow Cu(II)$ CT transitions can appear between 220–270 nm and 320–350 nm, and the $N^{-} \rightarrow Cu(II)$ transition can appear in the range 290–320 nm [15]. Therefore, the overall higher absorption in the 300–350 nm region for the Cu^{2+}-W48A/R129W azurin complex shown in Figure 2 confirms the binding of the copper ion to the 6xHis-tag.

3.3.2 Steady-state fluorescence

To investigate the changes in steady-state fluorescence intensity following metal-ion binding, the fluorescence spectra of WT, and W48A/R129W azurins engineered with the 6xHis-tag were measured in the presence of increasing concentrations of Cu^{2+}, Ni^{2+}, Zn^{2+} and Cr^{3+}. At pH 6.8, the imidazole groups of the His-tag are largely deprotonated and are therefore able to coordinate the metal ions in solution [15, 26, 30, 31], thus preventing precipitation of the corresponding hydroxides. Both the emission intensities of the buried Trp48 (Figure 4a) and of the exposed Trp129 in the R129W protein (Figure 4b) and in the W48A/R129W double mutant (Figure 4c) decrease with increasing metal-ion concentration. No significant changes in shape or position are observed in the first two cases, while in the latter the already noticed unquenched tyrosine emission, with maximum around 305 nm, becomes dominant at large metal-ion concentrations.

The normalized emission intensities of the mutant R129W azurin at 310 and at 350 nm are shown as functions of metal ion concentration in Figure 5. The emission intensities for the WT protein (at 310 nm) and the W48A/R129W mutant (at 350 nm) follow similar trends and are not reported.

The observed, sometimes extremely marked quenching cannot be due to radiative energy transfer, i. e., reabsorption of emitted fluorescence by the quencher, because of the extremely low absorbances of the His-tag/metal ion complexes in

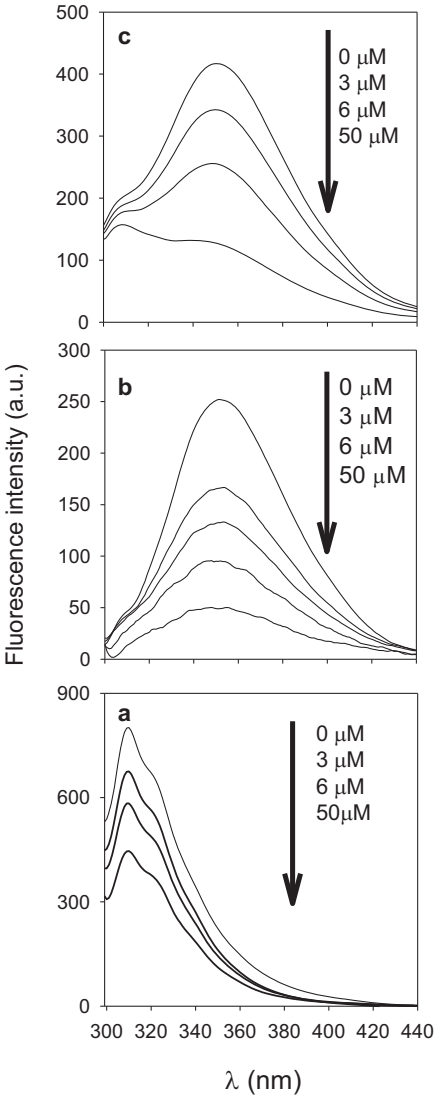

Figure 4: Fluorescence emission spectra of Trp48 in WT (a) and of Trp129 in R129W (b) and W48A/R129W (c) 6xHis-tag azurins in presence of increasing Cu^{2+} concentrations. Spectra were recorded at 293 K and at pH 6.8 using 3.0×10^{-6} M protein samples. The emission spectra of the Trp129 in the R129W mutant were obtained by subtracting the emission spectra of the WT protein from the total emission spectra of the mutant as reported in the text. $\lambda_{exc} = 295$ nm.

the spectral region of the tryptophan emission (see Figure 2). Thus, non-radiative processes are responsible for the observed quenching. The metal-ion-induced quenching percentages at 22 μM metal-ion concentrations (Table 3) show similar results for a given tryptophan residue in the two azurins that contain it. Cu^{2+} binding causes a more pronounced quenching of Trp129, 70–80%, than of Trp48, 40–50%, likely because of a larger distance of the latter donor from the 6xHis-tag/Cu^{2+} complex acceptor. All other ions cause a lower and similar quenching

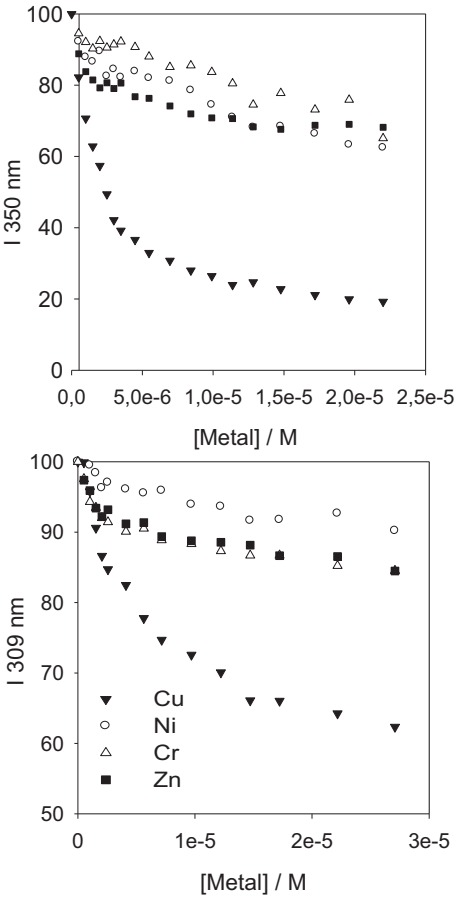

Figure 5: Emission intensities of Trp48 (top) and Trp129 (bottom) of the R129W mutant in the presence of increasing metal ion concentrations. Measurements were performed at 20 °C and pH 6.8

of the two tryptophans, 15–30%. Cr^{3+} is likely a better quencher than Ni^{2+} and Zn^{2+} because, at an added metal ion concentration 22 μM, its quenching efficiency is similar to the quenching efficiencies of these bipositive ions while, due to a markedly lower affinity for 6xHis-tagged azurins (see below), its titration is quite far from the endpoint. The higher quenching ability of the copper ion relative to the other bipositive metal ions correlates with the stronger absorption increase in the tryptophan emission region, 300–350 nm, due to the 6xHis-tag/Cu^{2+} complex formation (Figure 2), and likely results from a more favorable spectral overlap factor.

Table 3: Percentages of quenching of Trp48 and Trp129 fluorescence emission of WT, R129W and W48A/R129W 6xHis-tag azurins at 22 μM metal-ion concentration. The estimated errors are ± 15% on the Cu^{2+} values, ± 30% on the other ones.

	WT Trp48	R129W Trp48	R129W Trp129	W48A/R129W Trp129
Cu^{2+}	45	42	75	79
Ni^{2+}	15	18	20	3
Zn^{2+}	23	20	25	2
Cr^{3+}	16	19	30	20

Table 4: Affinity constants ($/10^5$ M) of Cu^{2+}, Ni^{2+}, Zn^{2+} and Cr^{3+} for WT, R129W and W48A/R129W 6xHis-tag azurins determined from quenching of Trp48 and Trp129 fluorescence emissions according to Equation (1). $T = 20\,^{\circ}C$. The confidence intervals within parentheses were obtained from the non-linear least-squares fittings.

	WT/Trp48	R129W/Trp48	R129W/Trp129	W48A/R129W/Trp129	Average values
Cu^{2+}	1.8(±0.5)	1.2(±0.8)	2(±0.8)	1.1(±0.7)	1.5
Ni^{2+}	0.4(±0.1)	0.4(±0.1)	1.5(±0.5)	2(±0.5)	1.1
Zn^{2+}	1.5(±0.5)	1.2(±0.5)	2.8(±0.7)	1.3(±0.2)	1.7
Cr^{3+}	0.003(±0.001)	0.1(±0.05)	0.005(±0.001)	0.007(±0.002)	0.005 *

* Calculated using the three more homogeneous results.

3.3.3 Metal ion-6xHis-tag azurin affinities

The affinity constants (K) of Cu^{2+}, Ni^{2+}, Zn^{2+} and Cr^{3+} for the three His-tagged proteins (Table 4) were determined by fitting the available steady-state fluorescence data to Equation (1) (examples are shown in Figure S2 of the supplementary material). The data could be well fitted using a 1 : 1 azurin 6xHis-tag/metal ion stoichiometry. All values for bipositive ions are of the order of $10^5\ M^{-1}$, corresponding to $\Delta G°$ values of about $-28\ kJ\ mol^{-1}$, and within the range typical of transient complexes [32]. The result for Cu^{2+}, $1.5(\pm 0.6) \times 10^5\ M^{-1}$ is in excellent agreement with the estimate obtained from time-resolved decay analysis (see below). The similarity of the binding constants for all bipositive ions clearly indicates that the 6xHis-tag has a similar, relatively high affinity towards all these metal ions, in agreement with literature data for the isolated hexapeptide-6xHis-tag [33, 34]. On the other hand, the K values for Cr^{3+} (approximately $5 \times 10^2\ M^{-1}$) are one-to-two orders of magnitude lower, corresponding to $\Delta G°$ values of about $-15\ kJ\ mol^{-1}$.

These results are consistent with the similar extractability data for Cu^{2+}, Ni^{2+} and Zn^{2+} ions by an alkylhistidine at pH 6.8 [35], and with the low efficiency of histidine with respect to other chelating agents to mobilize Cr^{3+} from a contaminated soil [36, 37]. The intermediate hard-soft base properties of imidazole correlates with its efficiency in coordinating metal ions with different hard-soft characteristics. Moreover, the 6xHis-tag, with its high number of metal-binding residues, turns out to be an extremely flexible chelating ligand able to coordinate metal ions with different dimensions and coordination geometries [15, 35].

3.3.4 Time-resolved fluorescence

Time-resolved measurements provide additional information on the effect of bound Cu^{2+} ion on the Trp48 and the Trp129 emissions (Table 2). Quenching of the Trp48 emission is immediately apparent from a comparison of the amplitude-weighted lifetimes of WT azurin in the presence and absence of the added copper ion, 0.5(±0.1) vs 2.5(±0.4) ns (Table S1). The ratio of these lifetimes, 0.2(±0.05), corresponds to the ratio of the quantum yields [1] and, thus, to a quenching efficiency of about 0.8 at $[Cu^{2+}] = 50$ μM, slightly larger than the steady-state quenching efficiency extrapolated at saturation, about 0.6. In the presence of 50 μM Cu^{2+} ion, the intensity at $t = 0$ of the unquenched, 4.6 ns Trp48 decay contribution in WT azurin is about 7 times smaller (0.003–0.004 vs 0.022–0.023) than in the absence of added copper ion. Because sample absorbances, excitation intensities and detection experimental parameters were kept the same in all experiments, this ratio represents an estimate of the product of the ratio of the concentrations of copper-free 6xHis-tags without and with added copper ion times the ratio of the acquisition times of the experiments run with/without Cu^{2+} ion. From the value of the latter, 1.3, we can estimate the above concentration ratio, CR_0, to hold ~9, and the binding constant, $K = (CR_0 - 1)/[Cu^{2+}]$ to be about $1.6 \times 10^5\ M^{-1}$.

Quenching of the 4.6 ns component of the WT azurin yields both a 2.5(±0.2) ns component, and a marked increase in the fractional contribution of the ~0.2 ns component. These correspond to quenching rate constants $k_{q1} = 2(\pm 0.4) \times 10^8\ s^{-1}$ and $k_{q2} = 5(\pm 2) \times 10^9\ s^{-1}$. The latter is similar to the rate constant for quenching of Trp48 emission by the T1-site-bound copper ion, and suggests a similarly close donor/acceptor proximity. The source of this component remains unknown. The former is of the same order of magnitude as the rate constant for Trp129 quenching by the T1-site-bound copper ion, $k_{q2}^{W48A/R129W}$. We assign these similar, low $10^8\ s^{-1}$ quenching rate constants to energy transfer across the protein, from Trp48 to the 6xHis-tag-Cu^{2+} complex and from Trp129 to the T1-Cu^{2+} complex (Figure 1).

Addition of the copper ion to the single-tryptophan, W48A/R129W azurin causes a decrease in the amplitude-weighted lifetime of the Trp129 residue 0.2(±0.1) vs 1.6(±0.4) ns, i. e., a ratio ~ 0.1. Similarly to the WT azurin case, from this data we estimate a quenching efficiency of about 0.9 at $[Cu^{2+}] = 50\ \mu M$, consistent with the steady-state quenching efficiency at saturation, 0.90, and somewhat larger than the quenching efficiency of Trp48 emission by the added Cu^{2+} ions. Consistently with steady-state observations, more pronounced quenching of the Trp129 emission decay relative to that of Trp48 by the His-tag-bound copper ion is consistent with a shorter distance between the His-tag and the former residue relative to the latter one, and represents evidence of copper-ion binding at this site.

Overall, both the long (3.7(±0.3) ns) and the intermediate-lifetime (1.7(±0.2) ns) components of the R129W/Trp129 azurin emission decays are quenched by the bound Cu^{2+} ion, while the shortest lifetime in a three-component description decreases from 0.3 to about 0.15 ns and, in spite of this, its fractional contribution increases by a factor 6–7. It corresponds to quenching rate constants of $6(\pm1) \times 10^9\ s^{-1}$ a value consistent with close proximity of donor and acceptor, i. e., with quenching of Trp129 by the 6xHis-tag-Cu^{2+} complex. An intermediate lifetime of about 1 ns is found in our three-component description. It would correspond to quenching rate constants of $4 \times 10^8\ s^{-1}$ and $7 \times 10^8\ s^{-1}$ assuming it resulted from quenching of, respectively, the 1.7 or 3.7 ns lifetimes of the double mutant (Table 2). The observation of this poorly quenched emission component of Trp129 adds to those of the two previously unassigned components in the R129W/Trp129 and in the WT + Cu^{2+} decays to indicate the existence of additional conformations of the proteins or 6xHis-tag-Cu^{2+} complexation modes or positions.

Like with the 4.6 ns component of the WT azurin decay, we employ the amplitudes at $t = 0$ of the 3.7 ns component of the R129W/Trp129 azurin decay, 0.011 and 0.0024, and the acquisition time ratio, 1.9, to estimate the ratio of the concentrations of copper-free 6xHis-tags without and with added copper, $CR_0 \sim 9$, and the Cu^{2+} ion binding equilibrium constant, $K \sim 1.6 \times 10^5\ M^{-1}$. This is identical to the equilibrium constant estimated for Cu^{2+} ion binding to the 6xHis-tag WT azurin.

As a consequence of Cu^{2+} ion binding, the two-tryptophan R129W azurin mutant exhibits a decrease in the amplitude-weighted lifetime that somewhat depends on the emission wavelength, as expected for a decay resulting from two independent fluorophores with different emission spectra. The ratio holds 0.15 at 320 nm, 0.18 at 330 and 350 nm, 0.21 at 370 nm. The corresponding quenching efficiencies are between 0.79 and 0.85 and are consistent with the measured steady-state values. Their increase with increasing emission wavelength confirms

the more efficient quenching by the bound copper ion of the exposed Trp129 relative to buried Trp48. Although a four-exponential decay analysis contains too many fitting parameters to allow us to consider the results of the R129W + Cu^{2+} decay analysis unique, yet we obtained very good fits when using the lifetimes obtained from the decay analyses of the two single-tryptophan azurins in the presence of Cu^{2+}, 1.0 and 2.5 ns as fixed parameters. We therefore believe the most complex case analyzed, R129W with added Cu^{2+} ions, to be well described as an emission-wavelength dependent superposition of the decays of the two single-tryptophan azurins with added copper ion.

The features of tryptophan emission quenching processes by 6xHis-tag/Cu^{2+} complexes (HT-Cu) and their structural significance are summarized in the lower rows of Table 2 and are depicted in Figure 1.

4 Summary and concluding remarks

Trp48 and Trp129 emissions of WT, R129W and W48AR129W azurins are quenched as a consequence of metal-ion binding to C-terminal fused 6xHis-tags. The quenching efficiencies of both tryptophans show a marked dichotomy between Cu^{2+} and the other tested ions. Steady-state and time-resolved measurements indicate the copper ion to quench as much as 90–95% of the Trp129 emission and about 60–80% of the Trp48 emission in each of the proteins that contain these residues, in keeping with the smaller distance of the latter residue from the 6xHis-tag binding site of the added ions. Nickel and zinc ions exhibit lower steady-state quenching efficiencies, around 30%, all similar to each other. This difference between the effect of Cu^{2+} and those of the other ions correlates with the higher spectral overlap between the Cu^{2+}-6xHis-tag complex absorption and the Trp emission.

Time-resolved experiments indicate a more complex quenching rate constant landscape than expected for unique protein conformations or single Cu^{2+} binding sites. Low 10^8 s^{-1} rate constants are found for energy transfer across proteins, from Trp129 to the T1-site/Cu(II) complex and from Trp48 to 6xHis-tag/Cu^{2+} complexes. The 5×10^9 s^{-1} rate constant found in the WT decay is attributed to Trp48 to T1-site/Cu(II) complex energy transfer. A similarly high rate constant is deduced from the emission decay of W48AR129W with added Cu^{2+} ion, and is attributable to Trp129/6xHis-tag/Cu^{2+} complex energy transfer. However, a 2.7×10^9 s^{-1} quenching rate constant is found in the emission decay of this protein without added ions and clearly indicates that a much faster quenching is operative than expected from the distance between residue 129 and the T1-site in

the WT azurin XRD structure. Similarly unassigned on the basis of simple structural assumptions are a 5×10^9 s^{-1} and a $4-7 \times 10^8$ s^{-1} quenching rate constants found from analysis of the decay of, respectively, the WT and the doubly mutated azurin in the presence of added copper ions.

The amplitude-weighted lifetimes represents a useful overall, time-resolved observable to monitor Cu^{2+} binding to these 6xHis-tagged azurins. The ratio of these lifetimes in the presence and absence of added copper ions, 0.2(±0.05) for the WT azurin, ~ 0.1 for W48A/R129W azurin, between 0.15 and 0.21 (wavelength dependent) for R129W azurin, testifies of the sensitivity of this observable and confirms the higher quenchability of Trp129 by bound copper-ion relative to Trp48.

The 6xHis-tag features a relatively high affinity for all the bipositive metal ions studied and a one-order-of-magnitude lower one for Cr^{3+}. If combined with the known ability of azurin to cross cellular membranes, this observation suggests 6xHis-tagged azurins to be employed as reversibly-bound carriers of metal ions in physiological conditions. To this aim, improvement of coordination selectivity versus bipositive metal ions might be recovered by changing the composition of the His-tag, as its metal-binding properties change with the number of histidine residues and their spacing [34]. On the other hand, metal-ion signal selectivity, already achieved for Cu^{2+} in the present work, might be more finely and specifically modulated by careful analysis of donor/acceptor spectral overlap. In particular, given the absorption spectrum of a specific metal-ion/6xHis-tag complex, a fluorophore featuring an emission spectrum more specifically matching that absorption might be chemically tagged to a His-tag-fused azurin. We are presently considering such an extension of this introductory work.

Overall, using these his-tagged azurins as a test case, we have shown that bipositive metal ions bound at a suitable polyhistidine tail can be efficient tryptophan emission quenchers. Insertion of an additional tryptophan residue near the polyhistidine tag has added new, spectroscopically distinguishable fluorescence observables. This new machinery, extended to any protein of interest, can be employed in *in-vitro* label-free experiments aiming at characterizing the interactions of this protein with small ligands or a biological macromolecule. It enables a broadening of the range of fluorometric observables and thereby offers additional experimental opportunities to monitor structural changes involving protein regions containing the signaling tryptophan(s) or the terminal polyhistidine region. Furthermore, definition of a tryptophan-to-metal ion/His complex energy transfer path network lays the basis to identify such structural changes.

Acknowledgement: This work has received funding from the European Union's Seventh Framework Programme for research, technological development and

demonstration under the grant agreement n° 603240 (NMTrypI – New Medicine for Trypanosomatidic Infections), http://www.nmtrypi.eu/.

References

1. J. R. Lakowicz, *Principles of Fluorescence Spectroscopy*, 3rd edn., Springer, Berlin/Heidelberg (2006).
2. Y. Engelborghs, Spectrochim. Acta A **57**(2001) 2255.
3. Y. Engelborghs, J. Fluoresc. **13** (2003) 9.
4. A. Hawe, M. Sutter, and W. Jiskoot, Pharm. Res. **25** (2008) 1487.
5. A. Messerschmidt, R. Huber, T. Poulos, and K. Wieghardt, *Handbook of Metalloproteins*, Wiley, Chichester (2001).
6. A. Finazzi-Agrò, G. Rotilio, L. Avigliano, P. Guerrieri, V. Boffi, and B. Mondovì, Biochemistry **9** (1970) 2009.
7. A. G. Szabo, T. M. Stepanik, D. M. Wayner, and N. M. Young, Biophys. J. **41** (1983) 233.
8. G. Gilardi, G. Mei, N. Rosato, G. W. Canters, and A. Finazzi-Agrò, Biochemistry **33** (1994) 1425.
9. J. E. Hansen, J. W. Longworth, and G. R. Fleming, Biochemistry **29** (1990) 7329.
10. G. Mei, A. Di Venere, E. Nicolai, N. Rosato, and A. Finazzi Agrò, J. Fluoresc. **13** (2003) 33.
11. C. M. Hutnik and A. G. Szabo, Biochemistry **28** (1989) 3935.
12. S. J. Kroes, G. W. Canters, G. Gilardi, A. van Hoek, and A. J. W. G. Visser, Biophys. J. **75** (1998) 2441.
13. L. Fuentes, J. Oyola, M. Fernandez, and E. Quiñones, Biophys. J. **87** (2004) 1873.
14. M. Di Donato and B. Sarkar, Biochim. Biophys. Acta **1360** (1997) 3.
15. J. Watly, E. Simonovsky, R. Wieczorek, N. Barbosa, Y. Miller Y, and H. Kozlowski, Inorg. Chem. **53** (2014) 6675.
16. K. Terpe, Appl. Microbiol. Biotechnol. **60** (2003) 523.
17. D. S. Waugh, Trends Biotechnol. **23** (2005) 316.
18. D. Witkowska, R. Politano, M. Rowinska-Zyrek, R. Guerrini, M. Remelli, and H. Kozlowski, Chem. Eur. J. **18** (2012) 11088.
19. T. Yamada, A. M. Fialho, V. Punj, L. Bratescu, T. K. Das Gupta, and A. M. Chakrabarty, Cell. Microbiol. **10** (2005) 1418.
20. A. Alessandrini, C. A. Bortolotti, G. Bertoni, A. Vezzoli, and P. Facci, J. Phys. Chem. C **112** (2008) 3747.
21. T. Yamada, M. Goto, V. Punj, O. Zaborina, K. Kimbara, T. K. Das Gupta, and A. M. Chakrabarty, Infect. Immun. **70** (2002) 7054.
22. E. T. Adman and L. H. Jensen, Isr. J. Chem. **21** (1981) 8.
23. A. Riboldi-Tunnicliffe, N. W. Isaacs, and T. J. Mitchell, FEBS Lett. **579** (2005) 5353.
24. E. I. Solomon, J. W. Hare, D. M. Dooley, J. H. Dawson, J. H. Stephens, and H. B. Gray, J. Am. Chem. Soc. **102** (1980) 168.
25. M. A. Webb and G. R. Loppnow, J. Phys. Chem. A **103** (1999) 6283.
26. L. Casella and M. Gullotti, J. Inorg. Biochem. **18** (1983) 19.
27. M. Wynn, D. B. Knaff, and R. A. Holwerda, Biochemistry **23** (1984) 241.
28. D. J. Spira-Solomon and E. I. Solomon, J. Am. Chem. Soc. **109** (1987) 6421.

29. E. I. Solomon, U. M. Sundaram, and T. E. Machonkin, Chem. Rev. **96** (1996) 2563.
30. P. Deschamps, P. P. Kulkarni, and B. Sarkar, Inorg. Chem. **43** (2004) 3338.
31. V. G. Shtyrlin, Y. I. Zyavkina, E. M. Gilyazetdinov, M. S. Bukharov, A. A. Krutikov, R. R. Garipov, A. S. Mukhtarov, and A. V. Zakharov, Dalton Trans. **41** (2012) 1216.
32. S. Santini, A. R. Bizzarri, T. Yamada, C. W. Beattie, and S. Cannistraro, J. Mol. Recognit. **27** (2014) 124.
33. W. R. Kirk, Protein Expr. Purif. **95** (2014) 1.
34. S. Knecht, D. Ricklin, A. N. Eberle, and B. Ernst, J. Mol. Recognit. **22** (2009) 270.
35. H. Morizono, T. Oshima, and Y. Baba, Sep. Purif. Technol. **80** (2011) 390.
36. L. Jean, F. Bordas, and J.-C. Bollinger, Environ. Pollut. **147** (2007) 729.
37. A. E. Martell and R. M. Smith, *Critical Stability Constants*, Plenum Press, New York, London (1974).

Supplementary material: The online version of this article
(DOI: 10.1515/zpch-2015-0749) provides supplementary material for authorized users.